buildings

MDPI

Article

Geometry-Driven Parametric Modeling of Reinforcement in Variable-Section Special-Shaped Columns Using BIM

Yingjie Liu [1], Qinghe Liu [2], Hongmei Li [2,*] and Shushan Li [2,*]

[1] School of Water Conservancy, North China University of Water Resources and Electric Power, Zhengzhou 450046, China
[2] School of Civil Engineering and Communication, North China University of Water Resources and Electric Power, Zhengzhou 450046, China; z20241030348@stu.ncwu.edu.cn
* Correspondence: lihongmei@ncwu.edu.cn (H.L.); lishushan@ncwu.edu.cn (S.L.)

Abstract

Automated reinforcement modeling of variable-section special-shaped columns remains challenging because sectional variation simultaneously affects longitudinal-bar trajectories and stirrup configurations. This study proposes a geometry-driven parametric BIM method in which section dimensions and reinforcement-detailing parameters are mapped to reinforcement control points. Longitudinal bars in stable regions are represented by two endpoints, while those crossing the transition region are described using multi-control-point trajectories. Stirrup coordinates are updated with elevation to maintain geometric compatibility with inclined longitudinal reinforcement. The method was implemented in Autodesk Revit 2020 using C# and the Revit API and applied to L-, T-, cross-, and Z-shaped variable-section columns. Quantitative validation showed a mean spatial deviation of 0.161 mm across 264 representative control points, while the proposed workflow achieved a mean case-specific modeling-time reduction of 93.03% compared with conventional manual modeling. Reinforcement length and quantity outputs were also consistent with independent calculations. An engineering application further illustrated the use of the proposed workflow in a practical project context. The proposed framework provides an efficient and extensible approach for coordinated reinforcement generation and BIM-based information output in regular variable-section special-shaped columns.

Keywords: BIM; Revit API; parametric modeling; automated reinforcement detailing; variable-section special-shaped column

Check for updates

Academic Editor: Antonio Caggiano

Received: 3 September 2026
Revised: 15 October 2026
Accepted: 24 October 2026
Published: 27 October 2026

Copyright: © 2026 by the authors. Licensee MDPI, Basel, Switzerland. This article is an open access article distributed under the terms and conditions of the Creative Commons Attribution (CC BY) license.

1. Introduction

Building Information Modeling (BIM) has been widely adopted in the architecture, engineering, and construction industry to integrate geometric and non-geometric information throughout the building lifecycle [1,2]. In reinforced-concrete construction, BIM provides a three-dimensional digital environment for structural design, reinforcement detailing, constructability assessment, and construction coordination [3,4]. Compared with conventional two-dimensional drawings, BIM models can represent reinforcement geometry and spatial relationships more intuitively, which is particularly valuable for structural members with complex reinforcement configurations. However, reinforcement modeling still involves substantial repetitive operations, and the modeling process becomes increasingly difficult when the geometry of structural members changes along their height or when multiple reinforcement constraints must be satisfied simultaneously. Variable-section columns are a

representative case in which changes in cross-sectional geometry directly affect the positioning and trajectories of longitudinal rebars and stirrups, thereby increasing the difficulty of efficient and accurate BIM-based reinforcement detailing [5].

Recent research has progressively extended BIM from conventional geometric representation toward parametric, rule-based, and automated modeling. Parametric BIM methods have been developed for complex engineering structures and specialized components, demonstrating the potential of explicit geometric parameters for automated model generation [6–8]. At the component level, intelligent modeling and self-adaptive reinforcement plug-ins have shown that rule-based geometric relationships can reduce repetitive modeling operations and allow reinforcement geometry to respond automatically to changes in component dimensions [9,10]. Visual-programming approaches and parameterized reinforcement-generation methods have further expanded computational BIM workflows for geometrically complex structural components [11,12]. These studies indicate that BIM is increasingly functioning as a computational environment in which structural geometry can be generated and updated through explicit engineering rules.

In parallel with geometric automation, considerable attention has been given to reinforcement-layout optimization and spatial conflict resolution. BIM-based reinforcement optimization has been investigated for reinforced-concrete frames and floor systems [13,14]. Artificial-potential-field methods, Q-learning, and decomposed optimization algorithms have subsequently been introduced to improve reinforcement arrangement and resolve spatial conflicts [15–17]. More recent studies have incorporated evolutionary optimization and graph-based learning into automated reinforcement detailing [18,19], while two-stage optimization and learning-based approaches have been applied to generate clash-free reinforcement layouts [20,21]. These studies have substantially advanced reinforcement optimization and clash avoidance; however, their primary focus is generally on optimizing or adjusting reinforcement layouts after the host geometry and basic reinforcement configuration have been defined.

Beyond reinforcement-layout optimization, BIM-based reinforcement research has increasingly extended toward information interoperability, fabrication, computational modeling, and construction-process integration. Optimization methods have been combined with BIM to support reinforcement cutting-stock planning [22]. BIM-based structural workflows have also been applied to reinforcement detailing and quantity take-off [23], while related studies have emphasized interoperability and structured data management in structural BIM environments [24]. From the perspective of reinforcement information exchange, the requirements of BIM platforms across the concrete reinforcement supply chain have been investigated [25]. IFC-based approaches have subsequently been developed for automated rebar fabrication [26] and for integrating cut-and-bent reinforcement information throughout the supply chain [27]. More recent BIM-enabled workflows have further connected digital reinforcement information with automated reinforcement and robotic construction processes [28]. Visual-programming and computational-BIM studies have provided flexible mechanisms for translating engineering logic into executable modeling procedures [29,30], while research on rule classification has further supported the structured implementation of automated checking workflows [31]. BIM-based data-driven approaches have also been applied to reinforcement process and supply-chain management [32], and design–construction integration has been investigated to improve reinforcement-related cost and construction efficiency [33]. Together with foundational work on automated rule-based checking [34], these developments indicate that BIM is evolving from a visualization-oriented platform into a computational environment capable of supporting automated geometric generation, reinforcement-information integration, engineering rule implementation, fabrication, and downstream construction applications.

Reinforcement-specific downstream applications have meanwhile continued to develop. BIM-based intelligent approaches have been proposed for reinforcement-layout optimization in reinforced-concrete members [35], while automated bar-bending-schedule generation has improved the extraction and organization of reinforcement fabrication information [36]. BIM has also been introduced into intelligent reinforcement construction and model-based quantity calculation, strengthening information transfer from design to production [37,38]. At the fabrication stage, BIM–BVBS integration enables machine-readable reinforcement information to be transferred from BIM models to prefabrication processes [39]. Other studies have focused on reducing reinforcement cutting losses and material waste [40,41], while special-length and digital-twin-based strategies have extended BIM-supported reinforcement management toward procurement and construction control [42,43]. These studies have substantially advanced reinforcement information processing, fabrication support, and construction-oriented management. However, comparatively less attention has been given to the automatic geometric generation of reinforcement when sectional variation simultaneously affects longitudinal-bar trajectories and transverse-reinforcement boundaries.

Previous research has demonstrated the feasibility of applying BIM to reinforcement modeling for variable-section columns [5]. Related component-level studies have addressed prefabricated edge components [9], self-adaptive reinforcement [10], and non-uniform spiral reinforcement [12]. These studies demonstrate the feasibility of API- and rule-based reinforcement generation for variable-section or geometrically specialized structural components. However, the geometric problem addressed in the present study differs in that variations of the non-rectangular upper and lower sectional boundaries simultaneously affect the spatial trajectories of longitudinal reinforcement and the boundary geometry of transverse reinforcement.

According to JGJ 149-2017, special-shaped columns may adopt L-, T-, cross-, and Z-shaped sections [44]. For these members, sectional variation cannot be represented solely by updating isolated reinforcement positions because the same boundary change must be propagated consistently to both longitudinal-rebar trajectories and stirrup geometry within the transition region. The resulting problem therefore requires a unified formulation linking sectional boundaries, reinforcement control points, spatial trajectories, and elevation-dependent stirrup coordinates.

To address this problem, this study proposes a geometry-driven parametric reinforcement modeling method based on explicit boundary-to-control-point mapping. Reinforcement located in geometrically stable regions is represented by two endpoints, whereas reinforcement crossing the variable-section transition is described by multiple control points defining its piecewise spatial trajectory. The same sectional-boundary variation is further propagated to the stirrup boundary as a function of elevation, thereby coordinating longitudinal and transverse reinforcement within a common geometric framework.

The main contributions of this study are threefold. First, an explicit boundary-to-control-point mapping method is developed for longitudinal reinforcement in variable-section special-shaped columns, enabling sectional-boundary changes to be propagated directly to reinforcement trajectories. Second, an elevation-dependent stirrup-generation strategy is established in which the same sectional variation used to determine longitudinal-rebar trajectories is propagated to stirrup boundaries, thereby maintaining geometric coordination between longitudinal and transverse reinforcement. Third, the proposed framework is applied to L-, T-, cross-, and Z-shaped columns and integrated with Revit Schedule functions for reinforcement-information output and quantity take-off.

2. Methods

2.1. Development Environment and Overall Workflow

The proposed parametric reinforcement modeling method was implemented in Autodesk Revit 2020 using C# and the Revit API. All implementation and validation reported in this study were conducted in Revit 2020. The control-point geometry is computed independently of Revit-specific API calls; however, version-dependent interfaces, particularly those related to free-form reinforcement generation, may require adaptation when the workflow is migrated to newer Revit releases. A Windows Presentation Foundation (WPF) interface was developed for parameter input and model execution. The overall framework consists of four main stages: parameter definition, geometric computation, reinforcement generation, and reinforcement-information extraction.

As illustrated in Figure 1, the geometric parameters of the special-shaped column and the corresponding reinforcement-detailing parameters are first specified through the input interface. A local geometric reference system is then established, and the control-point coordinates of longitudinal rebars and stirrups are calculated according to the section geometry, concrete cover, reinforcement diameters, and detailing constraints. For reinforcement crossing the variable-section region, additional control points are introduced to describe the spatial transition between the lower and upper column sections. Stirrup boundaries within the same region are updated according to elevation so that their geometry remains coordinated with the inclined longitudinal reinforcement.

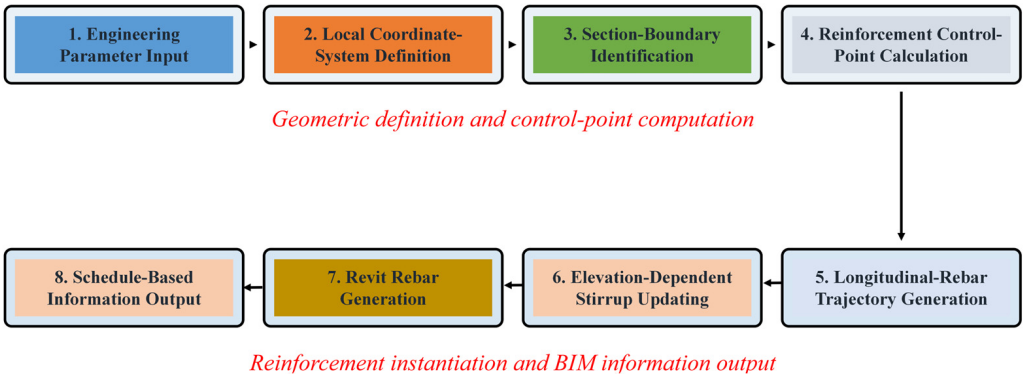


Figure 1. Overall workflow of the proposed parametric reinforcement modeling method.

The calculated reinforcement paths are subsequently converted into Rebar elements through the Revit API. After geometric generation, reinforcement attributes are organized through the Revit Schedule API to support quantity take-off and structured information output. The resulting workflow establishes a continuous process from engineering-parameter input to reinforcement geometry generation and BIM-based information extraction.

From the user perspective, interaction with the current implementation is primarily limited to specifying the required geometric and reinforcement-detailing parameters through the WPF interface and initiating model execution. Reinforcement control-point coordinates and individual three-dimensional trajectories are calculated internally and do not require manual definition by the user.

2.2. Parametric Definition and Coordinate-Based Geometric Framework

The proposed method adopts a parameter-driven representation of both column geometry and reinforcement detailing. The principal geometric parameters include the sectional dimensions of the lower and upper column segments, column height, beam–column joint dimensions, and the height of the variable-section transition region. Reinforcement-related

parameters include concrete cover, longitudinal-rebar diameter, stirrup diameter, anchorage- or lap-related dimensions, and stirrup spacing requirements. These parameters jointly define the geometric constraints used to determine reinforcement positions.

Conceptually, the workflow can be separated into a geometric-generation layer and a code-dependent detailing-rule layer. The geometric layer performs section-boundary identification, control-point calculation, trajectory construction, and stirrup-boundary updating, whereas the detailing-rule layer supplies code-dependent constraints such as concrete cover, reinforcement-spacing limits, anchorage or lap requirements, confinement provisions, and bending requirements. The present implementation adopts the Chinese detailing provisions used in this study; application under another regional standard would require the corresponding rule set to be redefined and validated.

A local Cartesian coordinate system is established for each special-shaped column. The column base is taken as the reference plane, with the horizontal coordinates describing reinforcement positions within the cross-section and the vertical coordinate representing elevation along the column height. Within this framework, reinforcement geometry is represented through calculable control points rather than manually positioned BIM elements. In the present implementation, sectional variation is resolved along the local X- and Y-directions, which is suitable for the regular variable-section geometries investigated in this study.

The geometric behavior of longitudinal reinforcement is distinguished according to whether the reinforcement is affected by sectional variation. Reinforcement located in geometrically stable regions is represented by start and end control points because its horizontal position remains unchanged along the relevant height. By contrast, longitudinal rebars passing through the variable-section transition require additional control points to describe the spatial change between the lower and upper sections. These points define a piecewise trajectory consisting of the corresponding vertical and inclined segments.

Stirrup geometry is treated within the same coordinate framework. In constant-section regions, the stirrup boundary remains unchanged and can be distributed vertically according to the prescribed spacing. Within the variable-section transition, however, the horizontal coordinates of the stirrup boundary are updated with elevation to accommodate the changing position of the inclined longitudinal reinforcement. This establishes a direct geometric relationship between sectional variation, longitudinal-bar trajectories, and stirrup boundaries.

Although the coordinate expressions differ among L-, T-, cross-, and Z-shaped columns because of differences in limb arrangement, sectional symmetry, and variation direction, the underlying computational sequence remains consistent: section-boundary identification, reinforcement control-point calculation, spatial trajectory construction, and stirrup-boundary updating. The detailed coordinate derivations are presented in Section 3.

To improve parameter consistency, discrete reinforcement parameters are restricted to predefined valid values within the graphical interface. This reduces the possibility of inconsistent inputs entering the subsequent coordinate calculations while retaining sufficient flexibility for different reinforcement configurations. The parameter-input interface is shown in Figure 2.

In the present implementation, sectional variation is resolved along the local X- and Y-directions, which is suitable for the regular variable-section geometries investigated in this study.

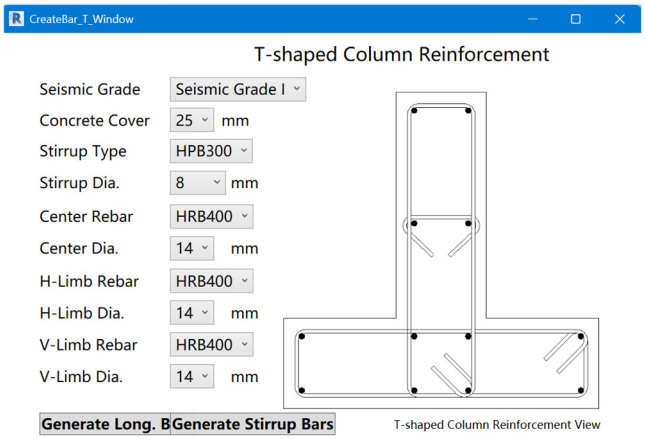


Figure 2. Graphical interface for parametric input of geometric and reinforcement-detailing parameters.

2.3. Revit API-Based Reinforcement Generation and Information Output

After the reinforcement control points have been determined, the corresponding geometric paths are constructed and converted into Rebar elements through the Revit API. Straight longitudinal reinforcement is generated from line segments defined by two control points, whereas reinforcement crossing the variable-section transition is constructed from piecewise paths connecting multiple control points. In this manner, changes in section geometry are transferred directly to the reinforcement trajectory through the calculated coordinates.

For reinforcement arrangements exhibiting geometric symmetry, representative bars are generated first and the remaining reinforcement is obtained through successive mirror operations, as illustrated for the T-shaped column. This symmetry operation is an optional computational strategy rather than a prerequisite of the control-point formulation. For a prescribed asymmetric reinforcement layout, the affected bars can instead be generated independently from their corresponding section boundaries and control-point coordinates without mirror replication.

Stirrups are generated from closed curves defined by the calculated boundary points. In constant-section regions, the same stirrup geometry is distributed vertically according to the prescribed spacing. Within the variable-section transition, the relevant boundary coordinates are recalculated at each elevation before the corresponding stirrup is created. Consequently, the stirrup geometry responds to the sectional transition together with the longitudinal reinforcement rather than being treated as an independent fixed profile.

Following reinforcement generation, the proposed workflow integrates BIM-based quantity extraction through the Revit Schedule API. The generated Rebar elements retain structured attributes including bar type, diameter, length, strength grade, and quantity. These attributes are retrieved programmatically and organized within a dedicated reinforcement schedule, thereby converting the generated geometric model directly into structured reinforcement information without repeated manual transcription.

This integration establishes a continuous information chain from section and reinforcement parameters to control-point calculation, Rebar generation, and quantity output. The resulting information can support reinforcement quantity take-off and material organization. In Section 4, the extracted reinforcement length and quantity are further compared with independently calculated values to evaluate the consistency between reinforcement geometry and BIM-based information output. The calculated control points may also provide a geometric basis for subsequent automated clash detection. Since consecutive control points explicitly define the centerline trajectory of each reinforcement bar, the resulting curves can be evaluated spatially against adjacent reinforcement and structural

components. By considering the nominal bar radius together with a prescribed clearance, potential conflicts can be identified using minimum-distance calculations, bounding-box screening, or solid-intersection tests. If a clash is detected, the affected control points can subsequently be treated as adjustable geometric variables and locally modified subject to concrete-cover, clear-spacing, anchorage, and sectional-boundary constraints. Thus, the control-point representation provides a direct geometric interface for future clash-detection and avoidance algorithms, although automated clash resolution is beyond the scope of the present study.

3. Parametric Generation of Reinforcement in Variable-Section Special-Shaped Columns

3.1. Longitudinal Reinforcement Generation

According to JGJ 149-2017, special-shaped columns may adopt L-, T-, cross-, and Z-shaped cross-sections. When the sectional dimensions vary along the column height, the longitudinal reinforcement exhibits different geometric behaviors depending on its position within the section. In this study, a T-shaped variable-section column is selected as the representative case for deriving the coordinate relationships, and the same geometric principles are subsequently extended to the other section configurations.

According to the influence of sectional variation, the longitudinal reinforcement is classified into three categories: central longitudinal rebars, column-limb longitudinal rebars, and structural longitudinal rebars. Central longitudinal rebars are located in regions whose horizontal positions remain unchanged during the sectional transition and can therefore be represented by straight trajectories. Column-limb longitudinal rebars are directly affected by the dimensional variation between the lower and upper sections and require multiple control points to describe their spatial trajectories through the transition region. Structural longitudinal rebars are introduced where the spacing between adjacent principal rebars exceeds the allowable detailing limit. This classification provides the geometric basis for the coordinate formulations developed below.

3.1.1. Generation of Central Longitudinal Reinforcement

The central region of the representative T-shaped column is not directly affected by the sectional variation considered in this study. Consequently, the longitudinal reinforcement located in this region remains vertical and can be represented by two control points defining the lower and upper ends of the bar.

For a general central longitudinal rebar, the coordinate-determination process can be expressed as the following geometric mapping:

$$P_i = F(G, R)$$

where P_i denotes the control-point coordinates of the i-th reinforcement bar, G represents the geometric parameter set of the column and beam–column joint, and R represents the reinforcement-detailing parameter set. In the present study,

$$G = (b_1, h_1, b_2, h_2, h, H, H_n, h_c)$$

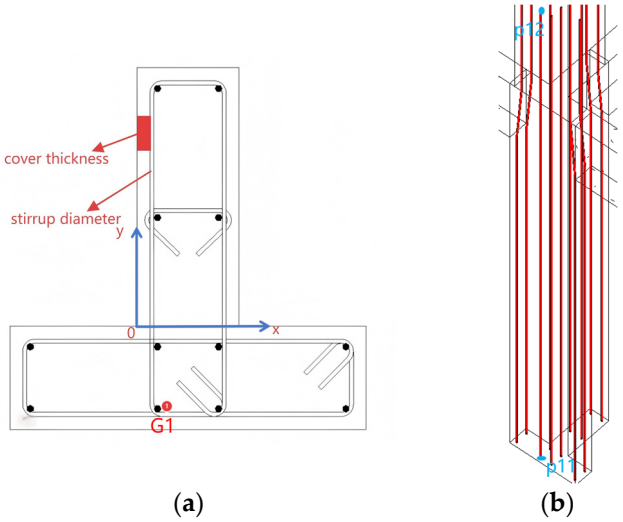
and

$$R = \left(c, d_g, d_l, l_{lE}\right)$$

where b_1 and h_1 denote the length and thickness of the horizontal limb of the T-shaped column, respectively; b_2 and h_2 denote the length and thickness of the vertical limb, respectively; h is the depth of the beam intersecting the column; H is the column height; H_n is

the clear height of the column; and h_c is the longer cross-sectional dimension of the column. The reinforcement-related parameters include the concrete cover thickness c, stirrup diameter d_g, longitudinal-rebar diameter d_l, and seismic lap length l_{lE} of the longitudinal tensile reinforcement.

Figure 3 illustrates the geometric arrangement and coordinate definition of the central longitudinal reinforcement. A T-shaped column is used as the representative case, and longitudinal rebar G1 is selected to demonstrate the coordinate-determination procedure.



(**a**) (**b**)

Figure 3. Geometric definition of central longitudinal reinforcement: (**a**) reinforcement arrangement; (**b**) control points of rebar G1.

The start and end control points of rebar G1 are denoted by p_{11} and p_{12}, respectively. The coordinates of p_{11} are expressed as

$$p_{11} = (x_1, y_1, z_1)$$

The position of the reinforcement centerline is governed by the concrete cover and the geometric relationship among the concrete boundary, stirrup, and longitudinal reinforcement. Therefore, the X-coordinate of the start point is

$$x_1 = c + d_g + \frac{d_l}{2} \tag{1}$$

Because the local coordinate origin is defined relative to the intersection of the horizontal and vertical limbs of the T-shaped cross-section, the Y-coordinate of G1 is determined from the lower boundary of the horizontal limb:

$$y_1 = -h_1 + c + d_g + \frac{d_l}{2} \tag{2}$$

The vertical coordinate of the start point is determined from the lower concrete boundary:

$$z_1 = c + d_g \tag{3}$$

The end point p_{12} represents the upper termination point of G1 after the reinforcement extends into the upper column. Because the central longitudinal reinforcement remains vertical and is not affected by the sectional transition, the horizontal coordinates of p_{11} and p_{12} remain unchanged:

$$x_2 = x_1$$

$$y_2 = y_1$$

and only the vertical coordinate varies.

To determine the upper termination point of the longitudinal rebar, an auxiliary vertical length L_c is introduced as:

$$L_c = \max(\frac{H_n}{6}, h_c, 500\ \text{mm})$$

The Z-coordinate of the upper control point is then calculated as:

$$z_2 = H + L_c + l_{lE} \tag{4}$$

For subsequent coordinate calculations, the effective offset from the concrete surface to the longitudinal-rebar centerline is defined as:

$$d_c = c + d_g + \frac{d_l}{2} \tag{5}$$

where c, d_g, and d_l denote the concrete cover thickness, stirrup diameter, and longitudinal-rebar diameter, respectively.

The coordinate solution is subject to three geometric constraints. The reinforcement centerline must satisfy the prescribed concrete cover, remain within the effective cross-sectional boundary after accounting for the stirrup diameter, and satisfy the applicable anchorage or lap-splice requirement at the upper termination. These constraints ensure that the calculated control points represent feasible reinforcement positions rather than purely geometric coordinates.

Using d_c, the two control points of G1 can be written compactly as

$$p_{11} = (d_c, -h_1 + d_c, c + d_g)$$

and

$$p_{12} = (d_c, -h_1 + d_c,\ H + L_c + l_{lE}$$

The resulting coordinates are summarized in Table 1.

Table 1. Coordinates of control points for central longitudinal rebar G1 in the T-shaped column.

Rebar	Point	X	Y	Z
G1	p_{11}	d_c	$-h_1 + d_c$	$c + d_g$
G1	p_{12}	d_c	$-h_1 + d_c$	$H + L_c + l_{lE}$

The remaining central longitudinal rebars are determined using the same geometric relationships, with their horizontal coordinates adjusted according to their positions within the T-shaped cross-section. Once the start and end points are obtained, each bar is represented by a straight line segment and subsequently converted into a Rebar element through the Revit API. The two-point formulation therefore constitutes the basic form of the coordinate-based representation; reinforcement affected by sectional variation requires additional control points, as described in Section 3.1.2.

3.1.2. Generation of Column-Limb and Structural Longitudinal Reinforcement

Unlike the central longitudinal reinforcement, longitudinal rebars located within the column limbs are directly affected by the dimensional difference between the lower and upper column sections. According to the reinforcement-detailing requirements for variable-section columns specified in 20G331-1 [45], longitudinal reinforcement within the column limb bends through the beam–column joint region before extending into the upper column, as shown in Figure 4. Based on this detailing requirement, the following coordinate relationships are derived geometrically from the section dimensions, reinforcement offsets,

and transition geometry. Consequently, the two-point representation used for central reinforcement is insufficient to describe the complete trajectory, and additional control points are required.

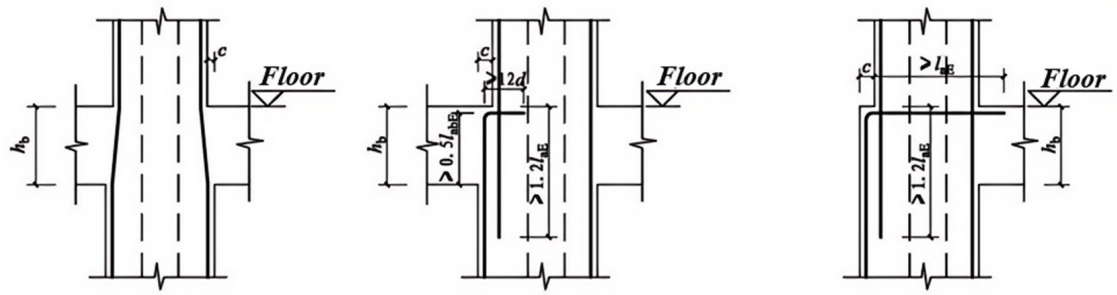
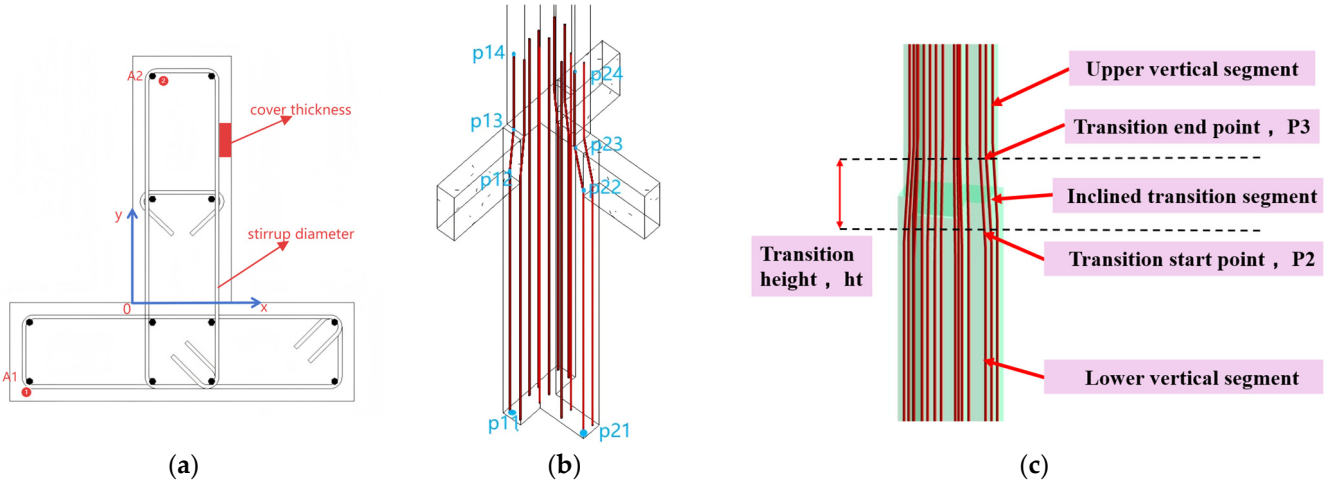


Figure 4. Longitudinal reinforcement detailing in the variable-section region of a column.

Taking the T-shaped column as the representative case, longitudinal rebar A1 is described by four control points p_{11}, p_{12}, p_{13}, and p_{14}, as shown in Figure 5. These points correspond to the lower starting point, the beginning of the sectional transition, the end of the transition, and the upper termination point, respectively. Connecting the four points sequentially produces a positionally continuous piecewise-linear trajectory consisting of a lower vertical segment, an inclined transition segment, and an upper vertical segment. The formulation ensures positional continuity at the segment junctions but does not impose tangent or curvature continuity; finite bending radii are not explicitly parameterized in the present model. For fabrication-oriented modeling, these junctions would additionally need to satisfy the minimum bend-radius requirements associated with the selected reinforcement grade, bar diameter, and applicable detailing standard.



(**a**) (**b**) (**c**)

Figure 5. Geometric definition of column-limb longitudinal reinforcement: (**a**) locations of representative longitudinal rebars in the T-shaped section; (**b**) control points and spatial trajectory of rebar A1. (**c**) Enlarged view of the longitudinal-rebar transition region.

For longitudinal rebar A1, the start point p_{11} is determined first. Based on the local coordinate system established previously, its X-coordinate is governed by the length of the horizontal limb, the thickness of the vertical limb, and the effective reinforcement offset d_c:

$$x_1 = -\frac{b_1 - h_2}{2} + d_c \tag{6}$$

where b_1 denotes the length of the horizontal column limb, h_2 denotes the thickness of the vertical column limb, and d_c is the effective offset defined in Equation (5).

The Y-coordinate of p_{11} is determined from the thickness of the horizontal limb:

$$y_1 = -h_1 + d_c \tag{7}$$

and its vertical coordinate is

$$z_1 = c + d_g \tag{8}$$

where h_1 is the thickness of the horizontal column limb.

The second control point p_{12} identifies the beginning of the variable-section transition. Because p_{11} and p_{12} coincide in horizontal projection, their X- and Y-coordinates remain unchanged, while only the vertical coordinate varies. The Z-coordinate of p_{12} corresponds to the clear height of the lower column:

$$z_2 = H_n \tag{9}$$

Thus,

$$p_{11} = (-\frac{b_1 - h_2}{2} + d_c, -h_1 + d_c, c + d_g)$$

and

$$p_{12} = (-\frac{b_1 - h_2}{2} + d_c, -h_1 + d_c,\ H_n)$$

The third control point p_{13} is located at the upper boundary of the variable-section transition. Let $\Delta b_1 = b_{1,l} - b_{1,u}$ denote the total width variation of the horizontal limb between the lower and upper sections, where the subscripts l and u denote the lower and upper sections, respectively. For the symmetric T-shaped configuration considered in this study, the dimensional variation is equally distributed between the two lateral boundaries; therefore, the displacement of the corresponding reinforcement boundary is $\Delta b_1/2$. Let Δh denote the vertical height of the transition region. Compared with p_{12}, the X-coordinate of p_{13} changes according to the sectional variation, whereas its Y-coordinate remains unchanged:

$$x_3 = -\frac{b_1 - h_2}{2} + d_c + \frac{\Delta b_1}{2} \tag{10}$$

The corresponding vertical coordinate is

$$z_3 = H_n + \Delta h \tag{11}$$

Therefore,

$$p_{13} = (-\frac{b_1 - h_2}{2} + d_c + \frac{\Delta b_1}{2}, -h_1 + d_c,\ H_n + \Delta h)$$

The segment between p_{12} and p_{13} represents the inclined portion of A1 within the variable-section region. Its horizontal displacement is governed by the dimensional difference between the lower and upper sections, whereas its vertical extent is governed by the transition height Δh. This establishes an explicit relationship between sectional variation and longitudinal-rebar trajectory.

The fourth control point p_{14} represents the upper end of A1 after the reinforcement passes through the transition region. Above p_{13}, the reinforcement becomes vertical again; therefore, the horizontal coordinates of p_{13} and p_{14} remain identical, and only the Z-coordinate changes. Using the extension-length requirement defined in Section 3.1.1,

$$z_4 = H + L_c + l_{lE} \tag{12}$$

where

$$L_c = \max(\frac{H_n}{6}, h_c, 500\ \text{mm})$$

and l_{lE} is the seismic lap length of the longitudinal tensile reinforcement. Accordingly,

$$p_{14} = (-\frac{b_1 - h_2}{2} + d_c + \frac{\Delta b_1}{2},\ -h_1 + d_c, H + L_c + l_{lE})$$

The four control points p_{11}–p_{14} therefore define the complete trajectory of rebar A1. The lower and upper segments remain vertical, while the intermediate segment responds to the sectional dimensional change. This four-point representation provides the additional geometric description required for longitudinal reinforcement passing through the variable-section transition.

The same control-point principle is applied to longitudinal rebar A2 located in the vertical limb. In the representative T-shaped configuration adopted here, the centerline of the horizontal limb is maintained, and its total width variation is therefore distributed symmetrically between the two lateral boundaries. For the vertical limb, the junction with the horizontal limb remains geometrically fixed, while the dimensional variation occurs at the free-end boundary. This variation pattern is adopted for the representative derivation rather than as a general requirement of the framework. Other asymmetric sectional variations can be accommodated by redefining the moving boundary and the corresponding displacement used in the control-point calculation.

Let $\Delta b_2 = b_{2,l} - b_{2,u}$ denote the change in vertical-limb length between the lower and upper sections. Consequently, the corresponding reinforcement boundary undergoes the full displacement Δb_2 in the Y-direction rather than $\Delta b_2/2$. Therefore, the X-coordinate of A2 remains unchanged, whereas its Y-coordinate varies according to the vertical-limb dimensional change. Following the labels shown in Figure 5, the four control points of A2 are p_{21}, p_{22}, p_{23}, and p_{24}, corresponding to the lower starting point, transition start, transition end, and upper termination point, respectively.

The calculated coordinates of A1 and A2 are summarized in Table 2.

Table 2. Coordinates of control points for representative column-limb longitudinal reinforcement in the T-shaped column.

Rebar	Point	X	Y	Z
A1	p_{11}	$-\frac{b_1-h_2}{2} + d_c$	$-h_1 + d_c$	$c + d_g$
A1	p_{12}	$-\frac{b_1-h_2}{2} + d_c$	$-h_1 + d_c$	H_n
A1	p_{13}	$-\frac{b_1-h_2}{2} + d_c + \frac{\Delta b_1}{2}$	$-h_1 + d_c$	$H_n + \Delta h$
A1	p_{14}	$-\frac{b_1-h_2}{2} + d_c + \frac{\Delta b_1}{2}$	$-h_1 + d_c$	$H + L_c + l_{lE}$
A2	p_{21}	d_c	$b_2 - h_1 - d_c$	$c + d_g$
A2	p_{22}	d_c	$b_2 - h_1 - d_c$	H_n
A2	p_{23}	d_c	$b_2 - h_1 - d_c - \Delta b_2$	$H_n + \Delta h$
A2	p_{24}	d_c	$b_2 - h_1 - d_c - \Delta b_2$	$H + L_c + l_{lE}$

The coordinate expressions in Table 2 reveal a common directional pattern. Sectional variation of the horizontal limb is transferred primarily to the X-coordinate of A1, whereas variation of the vertical limb is transferred primarily to the Y-coordinate of A2. The same coordinate-based framework can therefore accommodate different reinforcement trajectories by identifying the affected section boundary and its corresponding update direction.

After the representative reinforcement trajectories have been determined, the geometric symmetry of the T-shaped cross-section is used to generate the remaining longitudinal rebars. Representative reinforcement is first generated directly from the calculated control points. Successive mirror operations are then performed about the predefined symmetry axes, as illustrated in Figure 6. This strategy reduces repeated coordinate calculations while preserving geometric consistency among symmetrically distributed rebars.

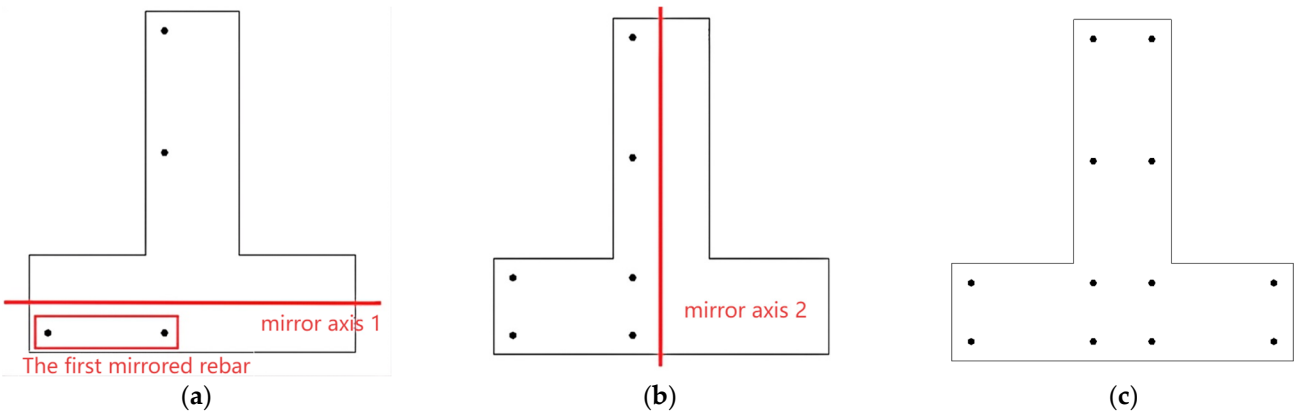


Figure 6. Symmetry-based generation of longitudinal reinforcement: (**a**) representative reinforcement before mirroring; (**b**) reinforcement after the first mirror operation; (**c**) completed reinforcement after the second mirror operation.

In addition to the principal longitudinal reinforcement, structural longitudinal reinforcement is introduced when the spacing between adjacent force-bearing longitudinal rebars exceeds the applicable detailing limit. According to Article 6.2.3 of JGJ 149-2017 [44], the spacing of longitudinal reinforcement should not exceed 200 mm for seismic Grades I, II, and III, 250 mm for Grade IV, and 300 mm for non-seismic design. Where these requirements cannot be satisfied by the principal reinforcement alone, additional structural longitudinal rebars with a diameter of not less than 12 mm are provided.

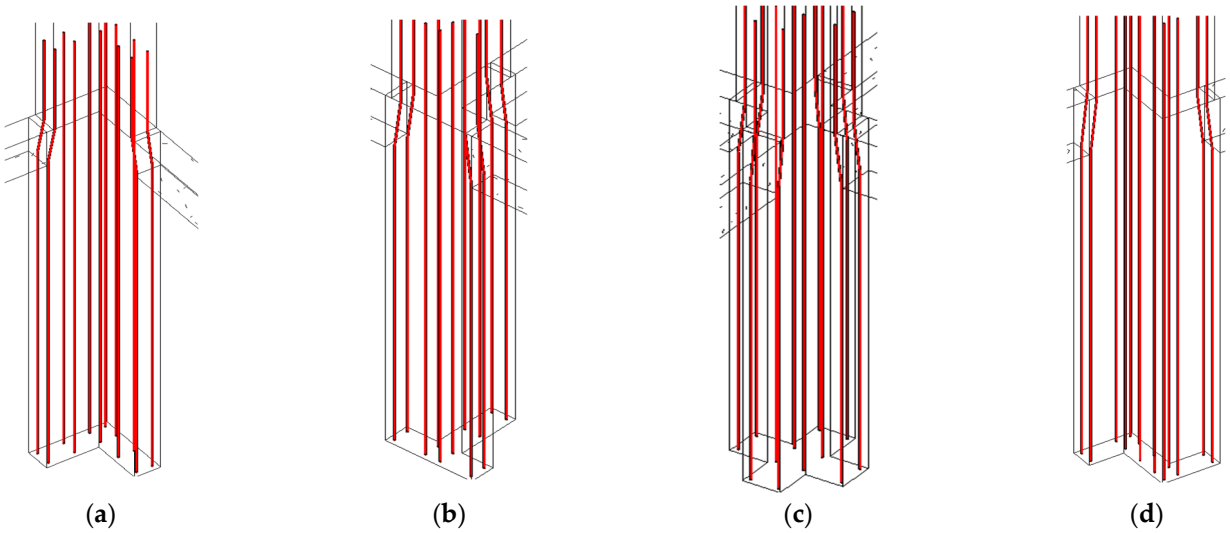
The positions of the additional structural rebars are determined using the same coordinate-based principle. After the effective reinforcement boundary is established from the concrete cover, stirrup diameter, and longitudinal-rebar diameter, the available spacing between adjacent principal rebars is evaluated. Where the allowable spacing is exceeded, additional reinforcement is introduced within the corresponding column limb, and its control-point coordinates are calculated from the local section geometry and reinforcement-spacing requirements.

Once all required control points have been determined, the points associated with each longitudinal rebar are connected sequentially to construct the corresponding reinforcement path. Straight reinforcement is generated from two control points, whereas reinforcement passing through the variable-section region is generated from four control points defining the lower vertical segment, inclined transition segment, and upper vertical segment.

Although the T-shaped column is used for the detailed coordinate derivation, the same geometric procedure is applied to the L-, cross-, and Z-shaped columns considered in this study. The relevant section boundaries, symmetry relationships, and coordinate-update directions are adjusted according to the corresponding section geometry, while the underlying sequence of control-point determination and trajectory construction remains unchanged. The resulting longitudinal reinforcement models for the four section types are shown in Figure 7.

3.2. Adaptive Generation of Stirrups in the Variable-Section Region

Compared with longitudinal reinforcement, stirrup generation in the variable-section region involves an additional geometric constraint. In a constant-section column, stirrups at different elevations have identical planar geometry and can therefore be generated by vertically replicating a predefined closed reinforcement curve. In the variable-section region, however, the longitudinal reinforcement is inclined between the lower and upper column sections. Consequently, the stirrup boundary must vary with elevation to maintain the required geometric relationship with the longitudinal reinforcement.



(**a**) (**b**) (**c**) (**d**)

Figure 7. Generated longitudinal reinforcement models: (**a**) L-shaped column; (**b**) T-shaped column; (**c**) cross-shaped column; (**d**) Z-shaped column.

In the proposed method, each closed stirrup considered in the coordinate calculation is represented by four control points connected sequentially to form a closed reinforcement curve. Figure 8 illustrates the geometric definition of a representative stirrup in the variable-section region of a T-shaped column. Following the labels shown in the figure, the four control points are denoted by A1, A2, A3, and A4. Their coordinates are determined from the sectional dimensions, concrete cover thickness c, stirrup diameter d_g, and the dimensional variation between the lower and upper column sections.

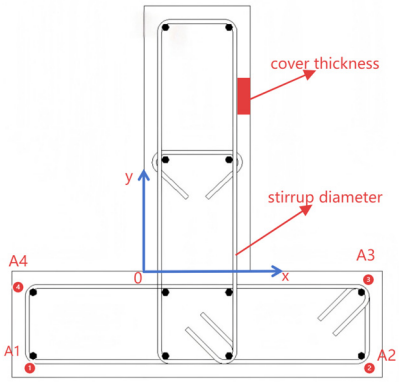


Figure 8. Geometric definition and control points of a stirrup in the variable-section region.

The uppermost stirrup within the variable-section region is selected as the reference stirrup. Its elevation corresponds to the upper boundary of the transition region:

$$z = H_n + \Delta h$$

where H_n denotes the clear height of the lower column and Δh denotes the vertical height of the variable-section transition. Because the stirrup centerline must satisfy the specified concrete cover, its effective offset from the concrete boundary is expressed as $c + \frac{d_g}{2}$. Taking the horizontal column limb of the T-shaped section as the representative case, the coordinates of A1–A4 for the uppermost reference stirrup are summarized in Table 3.

Table 3. Coordinates of the control points of the uppermost stirrup in the variable-section region of the T-shaped column.

Point	X	Y	Z
A1	$-\frac{b_1-h_2}{2}+c+\frac{d_g}{2}+\frac{\Delta b_1}{2}$	$-h_1+c+\frac{d_g}{2}$	$H_n+\Delta h$
A2	$-\frac{b_1-h_2}{2}+c+\frac{d_g}{2}+\frac{\Delta b_1}{2}$	$-c+\frac{d_g}{2}$	$H_n+\Delta h$
A3	$\frac{b_1+h_2}{2}+c+\frac{d_g}{2}-\frac{\Delta b_1}{2}$	$-h_1+c+\frac{d_g}{2}$	$H_n+\Delta h$
A4	$\frac{b_1+h_2}{2}+c+\frac{d_g}{2}-\frac{\Delta b_1}{2}$	$-c+\frac{d_g}{2}$	$H_n+\Delta h$

Here, b_1 denotes the length of the horizontal column limb, h_1 denotes its thickness, h_2 denotes the thickness of the vertical column limb, and Δb_1 represents the sectional variation associated with the horizontal limb. Once the four control points have been determined, they are connected sequentially to form a closed stirrup curve, which is subsequently converted into a Rebar element through the Revit API.

The principal geometric problem is the generation of the remaining stirrups within the transition region. As the stirrup elevation changes, the corresponding horizontal boundary must change simultaneously because the associated longitudinal reinforcement is inclined. For the horizontal limb considered here, this variation is reflected primarily in the X-coordinate, whereas the corresponding Y-coordinate remains unchanged. Stirrup generation is therefore transformed from a simple vertical replication process into a coupled update of vertical and horizontal coordinates, as illustrated in Figure 9.

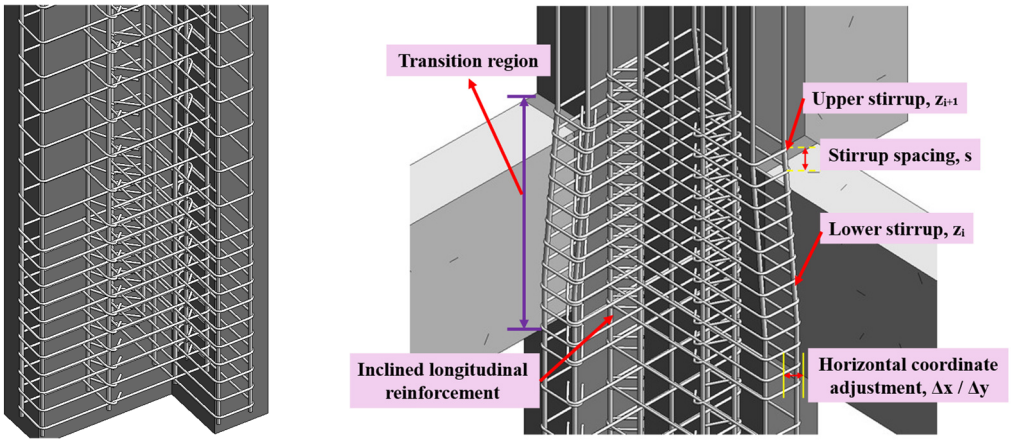


Figure 9. Elevation-dependent stirrup arrangement in the variable-section transition region: (**a**) overall arrangement; (**b**) enlarged view of adjacent stirrups and the corresponding horizontal boundary adjustment.

Let S_1 denote the maximum stirrup spacing in the confinement zone, Δb_1 the dimensional variation of the horizontal column limb, and Δh the height of the variable-section transition. For the symmetric T-shaped configuration considered in the derivation, the total dimensional variation is distributed between the two sides of the corresponding limb. Therefore, the horizontal increment applied during each stirrup-generation step is

$$\Delta x = \frac{\Delta b_1 S_1}{2\Delta h} \tag{13}$$

Equation (13) establishes a direct relationship among sectional variation, transition height, and stirrup spacing. Equation (13) is applied to the variable-section transition region, where the stirrup boundary must be updated with elevation to remain compatible

with the inclined longitudinal reinforcement. In the configuration investigated here, this transition is located within the confinement zone, and the corresponding confinement-zone spacing S_1 is therefore used in the incremental coordinate calculation. Once the sectional transition is completed, the sectional variation becomes zero and no further horizontal coordinate adjustment is required. When the elevation changes by one stirrup spacing S_1, the associated horizontal coordinate is adjusted by Δx. Thus, if the i-th stirrup is generated downward from the uppermost reference stirrup, its elevation is

$$z_i = H_n + \Delta h - iS_1 \tag{14}$$

The corresponding horizontal boundary coordinate is updated incrementally according to the direction of sectional variation. The sign of the horizontal increment depends on whether the relevant control point is located on the left or right boundary of the column limb. As a result, the stirrup boundary follows the changing position of the inclined longitudinal reinforcement rather than remaining vertically aligned with the uppermost stirrup. Equations (13) and (14) jointly define the elevation-dependent coordinate update of stirrups within the transition region. At each downward step, the Z-coordinate decreases by the prescribed stirrup spacing S_1, while the corresponding horizontal boundary coordinate is updated by Δx according to the direction of sectional variation.

The coordinate update is implemented iteratively. During each generation step, the Z-coordinate changes by the prescribed stirrup spacing, while the corresponding X-coordinate is updated according to Equation (13). The horizontal displacement is additionally constrained by the position of the longitudinal reinforcement associated with the stirrup boundary. Once this limiting position is reached, further horizontal displacement is terminated, preventing the stirrup from exceeding the intended geometric boundary.

Accordingly, successive stirrup positions can be interpreted as discrete samples of the longitudinal-reinforcement trajectory within the transition region. For a constant-section segment, $\Delta x = 0$, and the stirrup geometry remains unchanged with elevation. Within the variable-section segment, $\Delta x \neq 0$, and the horizontal coordinate is updated together with the vertical position. This distinction enables the same coordinate framework to represent both conventional constant-section stirrups and geometrically adaptive stirrups within the variable-section region.

For the vertical column limb, the same geometric principle is adopted, but the sectional variation is reflected in the Y-direction rather than the X-direction. Therefore, the Y-coordinate of the corresponding stirrup control points varies with elevation, whereas the X-coordinate remains unchanged. The incremental Y-direction displacement is determined from the dimensional variation of the vertical limb, transition height, and prescribed stirrup spacing using the same geometric relationship as that adopted for Δx.

After the control points at a given elevation have been calculated, A1–A4 are connected sequentially to form the corresponding closed stirrup curve. The curve is then converted into a stirrup element in Revit. Repeating this process through the prescribed confinement-zone height produces the complete stirrup arrangement in the variable-section region. Unlike conventional array-based generation, the relevant horizontal coordinates are recalculated before each stirrup is created, allowing the generated stirrup geometry to respond directly to the changing position of the longitudinal reinforcement.

Stirrups outside the transition region are generated using the same coordinate framework but do not require elevation-dependent horizontal adjustment because the column section remains constant. When the reinforcement arrangement changes from the confinement zone to the non-confinement zone, the stirrup spacing is updated according to the corresponding detailing requirements, whereas the planar stirrup geometry remains unchanged. The extent of the non-confinement region and the corresponding detailing requirements are determined according to Articles 6.2.10 and 6.2.12 of JGJ 149-2017 [44].

Although the T-shaped column is used to illustrate the detailed coordinate calculation, the same generation principle is applied to the L-, cross-, and Z-shaped columns. For each section type, the corresponding section boundaries and coordinate-update directions are identified first, after which the stirrup control points are calculated and converted into closed reinforcement curves. The resulting stirrup models for the four representative section types are shown in Figure 10.

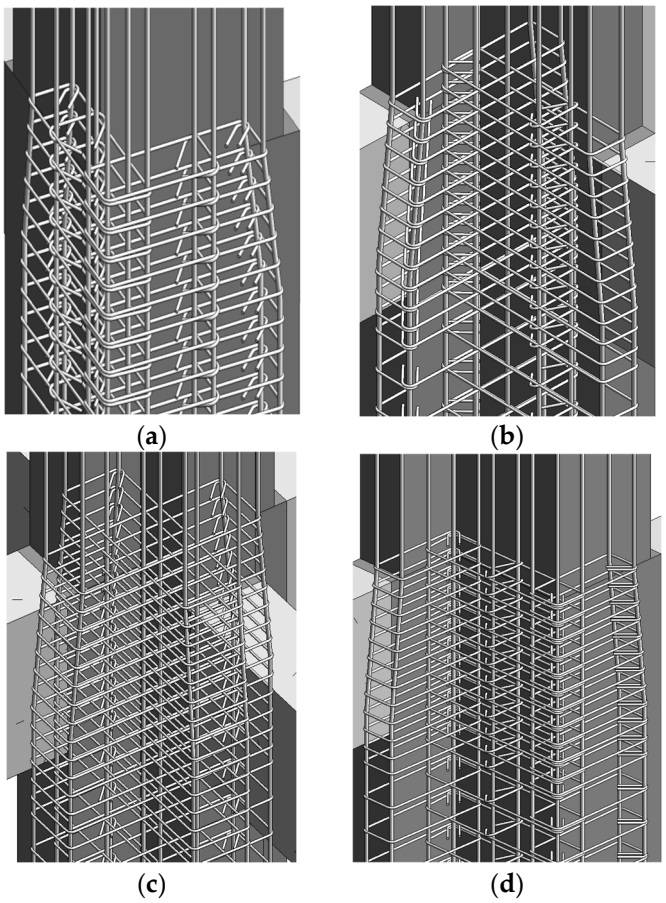


Figure 10. Generated stirrup models in the variable-section region: (**a**) L-shaped column; (**b**) T-shaped column; (**c**) cross-shaped column; (**d**) Z-shaped column.

The proposed stirrup-generation procedure establishes a direct geometric relationship between longitudinal-reinforcement trajectories and transverse reinforcement. The longitudinal reinforcement defines the changing spatial boundary within the variable-section region, while the stirrup coordinates are updated with elevation to follow this boundary. Thus, the geometric relationship between longitudinal reinforcement and stirrups is incorporated directly into the coordinate-calculation process, rather than treating the two reinforcement systems independently. This coupled representation forms the principal geometric feature of the adaptive stirrup-generation method.

4. Quantitative Validation and Engineering Application

To further evaluate the accuracy, modeling efficiency, and engineering applicability of the proposed geometry-driven parametric reinforcement modeling method, systematic validation was conducted based on the previously developed L-, T-, cross-, and Z-shaped variable-section special-shaped column models. Rather than relying solely on visual inspection of the generated three-dimensional reinforcement models, this section establishes quantitative comparisons among independently calculated results, reinforcement geom-

etry generated in Revit, conventional manual modeling, and reinforcement information output. The proposed method is therefore evaluated from four perspectives: geometric accuracy, modeling efficiency, consistency of reinforcement length and quantity, and engineering applicability.

The information flow of the proposed method can be summarized as follows. First, the control points of longitudinal rebars and stirrups are determined according to the column-section dimensions, concrete cover, reinforcement diameters, and relevant detailing parameters. The calculated control points are then converted into reinforcement curves and corresponding Rebar elements through the Revit API. Within the variable-section transition region, the trajectories of longitudinal rebars and the boundaries of stirrups are updated according to the direction of sectional variation and the corresponding elevation. Finally, reinforcement attributes, including bar type, diameter, length, strength grade, and quantity, are extracted and organized through the Revit Schedule API.

4.1. Validation Design and Evaluation Metrics

To investigate the applicability of the proposed method under different sectional configurations and parameter variations, three validation cases were established for each of the four representative variable-section special-shaped columns, namely L-, T-, cross-, and Z-shaped columns. A total of 12 validation cases were therefore considered.

The first group represents the baseline condition and is used to evaluate model-generation performance under representative sectional and reinforcement-detailing parameters. The second group represents an enhanced sectional-variation condition, in which the dimensional differences between the upper and lower sections are increased while the transition height is reduced. This configuration increases the inclination of longitudinal rebars within the transition region and provides a more demanding geometric condition for evaluating the control-point calculation method. The third group represents a reinforcement-detailing variation condition. Under this condition, the basic section geometry is maintained while the concrete cover, longitudinal-rebar diameter, stirrup diameter, and stirrup spacing are modified to examine whether detailing-parameter variations can be consistently propagated to the reinforcement control points and the resulting reinforcement geometry.

All validation cases adopt a total column height of 3600 mm and a clear lower-column height of 3000 mm. The transition height is 600 mm for the baseline and reinforcement-detailing variation cases and is reduced to 480 mm for the enhanced sectional-variation cases. The baseline reinforcement parameters include a concrete cover of 25 mm, longitudinal rebars with a diameter of 14 mm, stirrups with a diameter of 8 mm, and a stirrup spacing of 100 mm. For the reinforcement-detailing variation cases, these parameters are modified to 30 mm, 16 mm, 10 mm, and 80 mm, respectively. The detailed validation parameters are summarized in Table 4.

Across the validation matrix, the investigated sectional variation ranges from 100 to 150 mm in the local X-direction and from 80 to 125 mm in the local Y-direction, while the transition height ranges from 480 to 600 mm. These values represent dimensional differences between the corresponding upper and lower sectional boundaries rather than the complete sectional dimensions. The quantitative conclusions reported in this study are therefore limited to the investigated range of sectional variation and transition height. The enhanced sectional-variation cases provide a more demanding geometric condition within this range but should not be interpreted as exhaustive validation of arbitrarily extreme sectional transitions.

Table 4. Parameter settings for the 12 validation cases.

Case	Section Type	Transition Height/mm	ΔX/mm	ΔY/mm	Concrete Cover/mm	Longitudinal Bar Diameter/mm	Stirrup Diameter/mm	Stirrup Spacing/mm	Case Type
L-1	L-shaped	600	100	100	25	14	8	100	Baseline
L-2	L-shaped	480	125	125	25	14	8	100	Enhanced sectional variation
L-3	L-shaped	600	100	100	30	16	10	80	Detailing variation
T-1	T-shaped	600	120	80	25	14	8	100	Baseline
T-2	T-shaped	480	150	100	25	14	8	100	Enhanced sectional variation
T-3	T-shaped	600	120	80	30	16	10	80	Detailing variation
C-1	Cross-shaped	600	100	100	25	14	8	100	Baseline
C-2	Cross-shaped	480	125	125	25	14	8	100	Enhanced sectional variation
C-3	Cross-shaped	600	100	100	30	16	10	80	Detailing variation
Z-1	Z-shaped	600	120	100	25	14	8	100	Baseline
Z-2	Z-shaped	480	150	125	25	14	8	100	Enhanced sectional variation
Z-3	Z-shaped	600	120	100	30	16	10	80	Detailing variation

Here, ΔX and ΔY denote the dimensional differences between the upper and lower sections in the two principal horizontal directions. Although the local coordinate expressions differ among section types, the underlying geometric generation logic remains consistent. The program first identifies the section boundaries, limb directions, and symmetry relationships associated with reinforcement placement, and then determines the coordinate components affected by sectional variation. Variations in horizontal limbs are primarily represented by changes in the X-coordinate of the corresponding control points, whereas variations in vertical limbs are mainly represented by changes in the Y-coordinate.

Accordingly, different section types can share the same fundamental computational sequence: section-boundary identification, longitudinal-bar control-point determination, spatial trajectory construction, and stirrup-boundary updating.

The subsequent validation focuses on three quantitative aspects: geometric accuracy, modeling efficiency, and consistency of reinforcement information. An actual office-building project is further introduced to evaluate the engineering applicability of the proposed workflow.

4.2. Geometric Accuracy Validation

The core of the proposed parametric reinforcement modeling method is the transformation of section dimensions, reinforcement-detailing parameters, and variable-section geometric relationships into the control-point coordinates of longitudinal rebars and stirrups. Therefore, the consistency between independently calculated theoretical control points and the corresponding reinforcement geometry in Revit provides a direct measure of geometric modeling accuracy.

For each validation case, representative central longitudinal rebars, longitudinal rebars passing through the variable-section region, and stirrups within the transition region were selected for evaluation. For the central reinforcement, one representative bar was selected and its start and end points were examined, resulting in two control points. For longitudinal rebars passing through the variable-section region, two representative rebars affected by the principal sectional-variation direction were selected. Four control points were examined for each bar, corresponding to the lower start point, the transition start point, the transition end point, and the upper end point, giving eight control points in total. For stirrups, three representative elevations were selected at the lower, middle, and upper parts of the transition region, and four representative corner points were examined at each elevation, resulting in 12 control points.

Thus, 22 control points were examined for each case, producing a total of 264 representative geometric validation points for the 12 cases.

This sampling strategy covers the three principal geometric behaviors considered in the proposed method. Central longitudinal rebars are used to evaluate vertical positioning accuracy when the planar coordinates remain unchanged. Longitudinal rebars within the varying column limbs are used to evaluate how sectional variation is transferred to horizontal displacement and piecewise spatial trajectories. Stirrup control points at different elevations are used to assess the adaptive updating of the stirrup boundary according to the changing positions of the inclined longitudinal rebars.

The 264 points were selected using a geometry-behavior-based representative sampling strategy rather than random sampling. The objective was to cover the principal geometric behaviors of the proposed method rather than to exhaustively verify every reinforcement element and every control point.

For the i-th validation point, the geometric deviation is quantified as the Euclidean distance between the independently calculated reference coordinate and the corresponding coordinate extracted from the Revit model:

$$e_i = \sqrt{\left(x_i^R - x_i^C\right)^2 + \left(y_i^R - y_i^C\right)^2 + \left(z_i^R - z_i^C\right)^2} \tag{15}$$

where x_i^C, y_i^C, and z_i^C are the independently calculated coordinates of the i-th control point; x_i^R, y_i^R, and z_i^R are the corresponding coordinates in the Revit model; and e_i is the three-dimensional spatial deviation.

The geometric validation results for the 12 cases are summarized in Table 5.

Table 5. Geometric accuracy validation results for the 12 cases.

Case	Section Type	No. of Checked Points	Mean Spatial Deviation/mm	Maximum Spatial Deviation/mm	Positional Continuity of Longitudinal-Bar Trajectory	Geometric Compatibility of Stirrups
L-1	L-shaped	22	0.12	0.31	Pass	Pass
L-2	L-shaped	22	0.18	0.44	Pass	Pass
L-3	L-shaped	22	0.14	0.36	Pass	Pass
T-1	T-shaped	22	0.11	0.29	Pass	Pass
T-2	T-shaped	22	0.20	0.47	Pass	Pass
T-3	T-shaped	22	0.15	0.38	Pass	Pass
C-1	Cross-shaped	22	0.13	0.33	Pass	Pass
C-2	Cross-shaped	22	0.21	0.49	Pass	Pass
C-3	Cross-shaped	22	0.16	0.40	Pass	Pass
Z-1	Z-shaped	22	0.14	0.35	Pass	Pass
Z-2	Z-shaped	22	0.22	0.52	Pass	Pass
Z-3	Z-shaped	22	0.17	0.42	Pass	Pass
Overall	—	264	0.161	0.52	12/12 Pass	12/12 Pass

As shown in Table 5, the mean spatial deviation across the 12 validation cases ranges from 0.11 to 0.22 mm. The overall mean spatial deviation is 0.161 mm, and the maximum deviation among all representative control points is 0.52 mm. The baseline cases generally exhibit smaller deviations, whereas the enhanced sectional-variation cases show slightly larger values. This trend is associated with the larger sectional differences and reduced transition heights adopted in these cases, which produce greater changes in the coordinates of the transition-region control points.

The baseline cases generally exhibit relatively small geometric deviations. Among them, case T-1 presents the lowest mean spatial deviation of 0.11 mm and a maximum deviation of 0.29 mm.

When the sectional variation is intensified, the geometric deviations increase slightly. The mean spatial deviations of L-2, T-2, C-2, and Z-2 are 0.18, 0.20, 0.21, and 0.22 mm, respectively. Case Z-2 combines relatively large bidirectional sectional variations ($\Delta X = 150$ mm and $\Delta Y = 125$ mm) with a reduced transition height of 480 mm, producing the most pronounced coordinate changes among the Z-shaped cases. Consequently, small discrepancies between the independently calculated reference coordinates and the coordinates extracted from the Revit model are amplified at the transition-region control points. The resulting maximum deviation is 0.52 mm, which represents a localized worst-case discrepancy rather than a systematic geometric drift; the generated reinforcement trajectory remains continuous.

For the reinforcement-detailing variation cases, the mean spatial deviations of L-3, T-3, C-3, and Z-3 are 0.14, 0.15, 0.16, and 0.17 mm, respectively. These values lie between those of the baseline and enhanced sectional-variation cases. The results indicate that variations in concrete cover, longitudinal-bar diameter, stirrup diameter, and stirrup spacing can be propagated to the control-point coordinates without causing obvious amplification of geometric error.

In addition to coordinate deviations, the continuity of the generated reinforcement trajectories was examined. The central longitudinal rebars remained vertically aligned without abnormal horizontal offsets. Longitudinal rebars passing through the transition region consistently formed a lower vertical segment, an inclined transition segment, and an upper vertical segment in the predefined control-point sequence.

The stirrups within the variable-section region also remained geometrically compatible with the inclined longitudinal reinforcement. Their horizontal coordinates were continuously updated with elevation, and no evident local boundary crossing, reversed displacement, or abrupt geometric discontinuity was observed.

Overall, the geometric validation shows close agreement between the independently calculated control-point coordinates and the corresponding reinforcement geometry generated in Revit within the investigated range of section types and parameter variations. In all 12 cases, the longitudinal-rebar trajectories remained positionally continuous, and the stirrup boundaries remained geometrically compatible with the inclined longitudinal reinforcement. The reported mean and maximum deviations should be interpreted as sample-based statistics for the 264 representative control points rather than as absolute error bounds for every point in the generated reinforcement models. Additional sampling could modify the mean deviation and could identify a larger maximum deviation at locations not included in the present sample. From a modeling perspective, the observed deviations are sub-millimeter and are small relative to the detailing dimensions used in the validation cases, including concrete covers of 25–30 mm, longitudinal-bar diameters of 14–16 mm, stirrup diameters of 8–10 mm, and stirrup spacings of 80–100 mm. These results therefore indicate close geometric consistency between the independently calculated coordinates and the Revit-generated geometry; however, they should not be interpreted as construction tolerances, fabrication tolerances, or universal Revit acceptance limits.

4.3. Comparison of Modeling Efficiency

In addition to geometric accuracy, the engineering value of a parametric modeling method depends on its ability to reduce repetitive modeling operations. Conventional reinforcement modeling in Revit generally requires users to determine longitudinal-bar positions individually and manually adjust the bending positions of rebars passing through variable-section regions. For stirrups, the reinforcement boundary must also be adjusted according to the sectional geometry at different elevations. When section dimensions or reinforcement-detailing parameters are modified, these operations generally need to be repeated or rechecked.

The proposed method transforms this process into a rule-based workflow involving parameter input, control-point calculation, reinforcement-curve construction, and Rebar element generation. For symmetrically arranged longitudinal reinforcement, mirror operations can be used to reduce repeated coordinate calculations. For stirrups within the transition region, the corresponding horizontal coordinates are recalculated at different elevations.

To evaluate modeling efficiency, all 12 validation cases described in Section 4.1 were modeled using both conventional manual Revit modeling and the proposed parametric method. Identical section dimensions, reinforcement parameters, and final detailing requirements were adopted for both workflows. Both workflows were performed by the same operator, who had 5 years of experience in Revit-based reinforcement modeling. The manual workflow employed standard Revit reinforcement-modeling functions and included longitudinal-rebar creation and positioning, adjustment of transition trajectories, stirrup placement, and model checking. The parametric workflow included parameter input, control-point calculation, longitudinal-rebar generation, stirrup generation, and reinforcement-information output. The same timing definition was applied consistently to all 12 cases within each workflow. All timing tests were conducted on the same workstation equipped with a 13th Gen Intel(R) Core(TM) i7-13620H processor (2.40 GHz) and 16.0 GB of system memory, running 64-bit Windows 11 Home (Version 26H2). Autodesk Revit 2020 and the developed C# add-in were used under the same hardware and software environment for all validation cases.

The relative reduction in modeling time achieved by the proposed parametric method is calculated as:

$$R_t = \frac{T_m - T_a}{T_m} \times 100\% \tag{16}$$

where T_m is the modeling time required by the conventional manual Revit workflow, T_a is the modeling time required by the proposed parametric workflow, and R_t is the corresponding relative time reduction.

The results are summarized in Table 6.

As shown in Table 6, the parametric modeling time ranges from 48.6 to 61.5 s per case, whereas conventional manual modeling requires 612.4–961.4 s. Across the 12 validation cases, the average parametric and manual modeling times are 54.8 s and 792.8 s, respectively, and the mean of the case-specific time-reduction ratios is 93.03%.

Within the investigated cases, the parametric modeling time remained within a relatively narrow range of 48.6–61.5 s despite differences in section type and sectional variation. More complex limb arrangements and enhanced sectional variation generally increased the number of geometric calculations, but these operations were handled primarily through internal control-point recalculation rather than repeated manual repositioning. However, geometric complexity was not defined as an independent continuous variable in this study; therefore, the observed timing differences should be interpreted as descriptive workflow-level performance rather than as a general computational scaling relationship.

Table 6. Comparison of manual and parametric modeling efficiency.

Case	Section Type	Parametric Modeling Time/s	Manual Modeling Time/s	Time Reduction/%
L-1	L-shaped	48.6	612.4	92.06
L-2	L-shaped	52.3	701.8	92.55
L-3	L-shaped	50.1	648.7	92.28
T-1	T-shaped	51.4	734.5	93.00
T-2	T-shaped	56.7	842.9	93.27
T-3	T-shaped	53.6	781.2	93.14
C-1	Cross-shaped	55.2	823.6	93.30
C-2	Cross-shaped	61.5	961.4	93.60
C-3	Cross-shaped	58.1	887.3	93.45
Z-1	Z-shaped	53.9	768.2	92.98
Z-2	Z-shaped	59.8	914.6	93.46
Z-3	Z-shaped	56.4	836.9	93.26
Average	—	54.8	792.8	93.03

Note: The reported average time-reduction ratio is the arithmetic mean of the 12 case-specific reduction ratios.

The detailing-variation cases additionally provide an indicative assessment under denser reinforcement configurations. Relative to the corresponding baseline cases, the number of reinforcement elements increased by approximately 19.8–22.2%, whereas the measured parametric modeling time increased by approximately 3.1–5.3%. Because concrete cover, longitudinal-bar diameter, stirrup diameter, and stirrup spacing were modified simultaneously, these cases do not constitute an isolated reinforcement-density sensitivity test.

The individual validation cases contain 72–126 reinforcement elements. Across the 12 separately evaluated cases, a cumulative total of 1117 reinforcement elements was generated and verified. These elements were not processed simultaneously in one combined model; therefore, the reported timing results characterize component-level reinforcement generation rather than whole-building batch-processing performance.

4.4. Consistency Validation of Reinforcement Geometric Length and Quantity

Following the geometric-accuracy and modeling-efficiency evaluations, the reliability of the reinforcement information output was further examined. After reinforcement elements are generated, the developed program extracts and organizes reinforcement attributes through the Revit Schedule API, including bar type, diameter, length, strength grade, and quantity. This provides a continuous link between reinforcement geometry generation and structured information output.

To avoid validating Revit Schedule results against themselves, independently calculated reinforcement quantities were used as reference values. The geometric-length and quantity verification was performed for all 12 validation cases defined in Section 4.1. The independent reference calculations were performed using a spreadsheet-based calculation procedure outside the Revit Schedule extraction process. For straight longitudinal rebars, the theoretical length was calculated from the spatial distance between the start and end points. For rebars passing through the variable-section transition region, the lengths of the lower vertical segment, inclined transition segment, and upper vertical segment were calculated separately and then summed.

For stirrups, the length of an individual bar was independently calculated from the closed polygon formed by the corresponding control points at each elevation, after which the total length was obtained according to the number of stirrups. Reinforcement quantities were independently determined according to the longitudinal-bar layout rules, stirrup spacing, and reinforcement arrangement height.

The relative deviation between the reinforcement length extracted from the Revit Schedule and the independently calculated reference length is defined as:

$$E_L = \frac{| L_R - L_C |}{L_C} \times 100\% \quad (17)$$

where L_R denotes the total reinforcement length extracted from the Revit Schedule, L_C denotes the independently calculated reference length, and E_L denotes the relative length deviation.

The validation results are presented in Table 7. The reference values represent nominal geometric reinforcement lengths and bar counts; fabrication-specific bend deductions, couplers, and project-specific bar-bending adjustments are outside the scope of this verification.

Table 7. Comparison of independently calculated and Revit Schedule-derived reinforcement lengths and quantities.

Case	Section Type	Independently Calculated Geometric Length/m	Revit Schedule Geometric Length/m	Relative Length Deviation/%	Theoretical Quantity	Schedule Quantity	Quantity Deviation/%
L-1	L-shaped	248.36	248.48	0.048	72	72	0.00
L-2	L-shaped	252.91	253.11	0.079	75	75	0.00
L-3	L-shaped	276.44	276.62	0.065	88	88	0.00
T-1	T-shaped	315.72	315.86	0.044	86	86	0.00
T-2	T-shaped	322.84	323.11	0.084	89	89	0.00
T-3	T-shaped	349.16	349.39	0.066	103	103	0.00
C-1	Cross-shaped	382.47	382.65	0.047	104	104	0.00
C-2	Cross-shaped	391.38	391.76	0.097	108	108	0.00
C-3	Cross-shaped	426.23	426.55	0.075	126	126	0.00
Z-1	Z-shaped	301.65	301.80	0.050	82	82	0.00
Z-2	Z-shaped	309.74	310.02	0.090	85	85	0.00
Z-3	Z-shaped	337.58	337.85	0.080	99	99	0.00
Overall	—	3914.48	3917.20	0.069	1117	1117	0.00

As shown in Table 7, the independently calculated reinforcement lengths show close agreement with those extracted from the Revit Schedule. The relative length deviations for the 12 cases range from 0.044% to 0.097%, with a mean case-specific value of approximately 0.069%.

Among the investigated cases, T-1 exhibits the smallest relative length deviation of 0.044%, whereas C-2 exhibits the largest deviation of 0.097%. The enhanced sectional-variation cases generally show slightly larger deviations than the corresponding baseline cases because of the more complex inclined longitudinal-bar trajectories and elevation-dependent stirrup geometries. It is also noteworthy that the Revit Schedule length is slightly larger than the independently calculated geometric length in all 12 cases, indicating a small but systematic positive difference rather than randomly distributed numerical error. The present comparison does not isolate the individual contributions of Revit geometric representation, internal length evaluation, or numerical processing; therefore, the observed bias is reported without assigning it to a single implementation-level source. Nevertheless, the relative deviation remains below 0.1% for all cases.

For all 12 cases combined, the independently calculated reinforcement geometric length is 3914.48 m, whereas the corresponding Revit Schedule value is 3917.20 m, giving a positive difference of 2.72 m and an overall relative deviation of approximately 0.069%. In terms of reinforcement quantity, both the independently calculated result and the Revit Schedule contain 1117 bars in total, and the quantity deviation is 0% for all cases. The identical reinforcement counts indicate that no quantity-level omissions or duplicate elements were identified in the investigated validation cases.

The reinforcement-length and quantity validation further extends the role of the Schedule module from information organization to quantitative verification. Through this process, the proposed workflow establishes a continuous data chain from section and reinforcement parameters to control-point calculation, Rebar element generation, and structured reinforcement information output.

4.5. Engineering Case Application and Integrated Analysis

To further investigate the applicability of the proposed parametric modeling method under practical engineering conditions, an office-building project located in an airport economic zone of a city was selected as an engineering case study. The project is located southwest of the intersection of Fuliu Street and Daxue South Road, and Office Building A was selected as the research object.

Office Building A adopts a cast-in-place reinforced-concrete frame structural system and consists of three above-ground stories. The first-story height is 3.9 m, while the second- and third-story heights are both 3.6 m. The elevation difference between the indoor and outdoor ground levels is 0.3 m. The building has a structural safety grade of III and a design service life of 50 years. Its seismic fortification category is Class C, and the seismic design grade of the structural system is Grade III.

The engineering application follows the workflow of engineering-parameter acquisition, parametric input, control-point calculation, reinforcement generation, and information output. First, the column-section dimensions, column height, sectional-transition conditions, concrete cover, longitudinal-rebar diameter, and stirrup parameters are obtained from the structural drawings and reinforcement details. These parameters are then entered into the developed parametric modeling program. The control points of longitudinal rebars and stirrups are calculated according to the geometric relationships established in Section 3, after which the corresponding reinforcement elements are generated through the Revit API. Finally, reinforcement information, including bar type, diameter, length, and quantity, is organized through the Revit Schedule function.

For central longitudinal reinforcement in the engineering component, the planar coordinates remain unchanged because the reinforcement is not affected by sectional variation, and the bars therefore remain vertical along the column height. For longitudinal reinforcement located within varying column limbs, the required horizontal displacement is determined according to the dimensional difference between the upper and lower sections, producing a positionally continuous piecewise-linear trajectory consisting of a lower vertical segment, an inclined transition segment, and an upper vertical segment. Within the variable-section region, stirrup boundaries are recalculated according to elevation and the corresponding positions of the inclined longitudinal rebars, thereby maintaining geometric coordination between longitudinal and transverse reinforcement.

This engineering application is consistent with the unified modeling logic established for L-, T-, cross-, and Z-shaped columns. Although different special-shaped sections differ in limb arrangement, concave boundaries, sectional symmetry, and the direction of variation, they can be generated using the same fundamental geometric framework by modifying the relevant section boundaries and coordinate-update directions. Therefore, it is unnecessary to establish an entirely independent reinforcement-generation workflow for each section type.

The use of actual engineering parameters also demonstrates the model-updating capability of the proposed method. In conventional manual Revit reinforcement modeling, changes in column dimensions, concrete cover, or reinforcement diameters generally require the bending positions of longitudinal rebars, stirrup profiles, and their spatial relationships to be rechecked manually. In the proposed method, these relationships are explicitly represented through control-point coordinates determined by the section geometry and

reinforcement-detailing parameters. Consequently, when the input parameters are modified, the longitudinal-bar trajectories and stirrup boundaries can be recalculated automatically, transforming repeated local manual modification into a parameter-driven model update.

Combined with the validation presented in Sections 4.2–4.4, the engineering applicability of the proposed framework can be evaluated from three complementary aspects. First, geometric-accuracy validation examines whether the section and detailing parameters are correctly transformed into Revit reinforcement geometry. Second, the modeling-efficiency comparison evaluates the potential of the parametric method to reduce repetitive manual operations. Third, reinforcement-length and quantity validation determines whether the generated reinforcement geometry can be consistently transferred to structured reinforcement information.

The current framework nevertheless has a clearly defined range of applicability. It is primarily intended for regular L-, T-, cross-, and Z-shaped variable-section columns in which a clear correspondence exists between the upper and lower section boundaries and the section varies continuously along the column height. When column limbs are introduced or removed during the transition, or when the section undergoes other topological changes, the correspondence between the upper and lower boundaries must be redefined.

Curved transitions, free-form boundaries, and more complex three-dimensional sectional variations would require more general curve- or surface-based parametric representations. Mechanical reinforcement connections, highly congested beam-column joints, and multi-member intersections may also introduce additional spatial constraints and reinforcement clashes beyond the scope of the current geometry-generation framework. Future research may therefore integrate reinforcement-layout optimization, clash-resolution algorithms, and automated rule-checking procedures into the proposed method.

Overall, this section establishes a multi-level validation framework consisting of parameter-based validation cases, geometric-accuracy assessment, modeling-efficiency comparison, reinforcement-information consistency validation, and practical engineering application. For regular variable-section special-shaped columns, the proposed method provides a unified geometric logic for different section types and enables section dimensions and reinforcement-detailing parameters to be continuously propagated to longitudinal-bar control points, reinforcement trajectories, stirrup boundaries, and BIM attribute information. The introduction of an actual office-building project further establishes a direct connection between the proposed parametric modeling method and practical structural-engineering applications, providing a basis for its further use in complex reinforcement modeling and engineering information management.

5. Discussion

The validation results demonstrate that the proposed method can consistently generate coordinated reinforcement geometry for L-, T-, cross-, and Z-shaped variable-section columns within the investigated parameter range. The engineering relevance of these section types is supported by their explicit inclusion in JGJ 149-2017. However, the present study does not provide statistical evidence regarding the overall prevalence of variable-section special-shaped columns across the construction industry. Across 264 representative control points, the mean spatial deviation was 0.161 mm and the maximum deviation was 0.52 mm. In all 12 validation cases, the longitudinal-rebar trajectories remained positionally continuous and the stirrup boundaries remained geometrically compatible with the inclined longitudinal reinforcement. The largest deviation occurred locally in case Z-2 under the enhanced sectional-variation condition and did not indicate systematic geometric drift.

Compared with previous BIM-based reinforcement studies, the methodological contribution of this study lies in the explicit boundary-to-control-point mapping used to coordi-

nate reinforcement geometry under multidirectional sectional variation. Existing studies have demonstrated reinforcement optimization, intelligent layout, clash avoidance, quantity extraction, fabrication-oriented applications, and API-based generation for variable-section or geometrically specialized components [5,9,10,12,34,35]. The present method specifically addresses the coupled geometric response of longitudinal and transverse reinforcement to changes in non-rectangular sectional boundaries. Sectional variation is mapped directly to the control points defining longitudinal-rebar trajectories, while the same geometric change is propagated to stirrup boundaries as a function of elevation. Thus, the two reinforcement systems are coordinated within a common geometric framework rather than treated as independent generation tasks.

The integration of reinforcement generation with BIM information output further enables generated reinforcement geometry to be transferred directly into structured attributes such as bar type, diameter, geometric length, strength grade, and quantity. The geometric-length comparison showed relative deviations of 0.044–0.097%, with an overall value of approximately 0.069%, while the independently calculated and Schedule-extracted reinforcement counts were identical in all validation cases. The consistently positive Schedule-to-reference length differences indicate a small systematic difference between the analytical geometric-length calculation and the length representation used in the BIM environment, although the individual contributions of geometric representation and internal numerical processing were not isolated in this study. The present verification is limited to the nominal reinforcement geometry, geometric lengths, and bar counts represented in the BIM model. Prescribed anchorage- or lap-related dimensions explicitly incorporated into the reinforcement geometry are reflected in the corresponding model lengths; however, fabrication-specific constraints and adjustments—including grade- and diameter-dependent minimum bend radii, bend deductions, couplers, splice hardware, anchorage modifications not explicitly represented in the model, and project-specific bar-bending rules—require additional treatment before the generated reinforcement information can be used directly for fabrication.

The current framework has a clearly defined range of applicability and is primarily intended for regular variable-section special-shaped columns with clear correspondence between the upper and lower sectional boundaries. When column limbs are introduced, removed, or otherwise undergo topological changes, the corresponding boundary relationships must first be re-established. For curved, free-form, or arbitrarily oriented three-dimensional variations, the current Cartesian formulation would need to be generalized using local coordinate frames, vector-based displacement descriptions, and spline-, B-spline-, NURBS-, or surface-based boundary mapping. Curved transitions that preserve the same sectional topology may retain the existing boundary-correspondence concept but require curve-based trajectory and boundary representations. In contrast, topology-changing sections require a deeper extension because the sectional correspondence itself must be reconstructed, including boundary-feature identification and reinforcement-path assignment. The present implementation is deterministic and generates reinforcement geometry from prescribed design dimensions and detailing parameters; construction-induced dimensional and reinforcement-placement tolerances are not explicitly modeled. A formal robustness assessment would therefore require tolerance-based perturbation or uncertainty analysis of section dimensions, concrete cover, and reinforcement positions. In addition, the explicit control-point and centerline representation provides a geometric basis for future clash detection and constrained reinforcement adjustment, while adaptation to other design standards would require corresponding code-dependent cover, spacing, anchorage, confinement, and bending rules to be redefined and validated.

Accordingly, the proposed method should be regarded as a geometric instantiation framework rather than a replacement for structural analysis, reinforcement design, or comprehensive reinforcement optimization. Structural design determines the reinforcement configuration, while the proposed method converts the predefined configuration into coordinated BIM reinforcement geometry. Symmetry-based replication is optional: prescribed asymmetric layouts can be generated independently through their corresponding section boundaries and control-point coordinates, whereas load-dependent determination of asymmetric reinforcement demand, including that associated with eccentric loading, remains outside the scope of the present study. Future work may extend the framework to topology-changing and curved sections and integrate it with reinforcement optimization, automated rule checking, clash resolution, construction-tolerance assessment, and fabrication-oriented information workflows.

6. Conclusions

This study developed a geometry-driven parametric BIM method for reinforcement generation in variable-section special-shaped columns. By mapping sectional dimensions and reinforcement-detailing parameters to explicit control-point coordinates, the method establishes a unified geometric representation for longitudinal reinforcement and elevation-dependent stirrup generation in L-, T-, cross-, and Z-shaped columns.

Across 264 representative control points, the mean spatial deviation was 0.161 mm and the maximum observed spatial deviation was 0.52 mm. Compared with conventional manual Revit modeling, the average modeling time decreased from 792.8 s to 54.8 s, with a mean case-specific time reduction of 93.03%. Independent quantity verification further showed an overall reinforcement-length deviation of approximately 0.069%, while the independently calculated and Schedule-extracted reinforcement quantities were identical across all validation cases.

The current method is primarily applicable to regular variable-section special-shaped columns with clear correspondence between upper and lower sectional boundaries. Future work should extend the framework to topology-changing, curved, free-form, and more general three-dimensional transitions, as well as construction-tolerance assessment, complex reinforcement connections, automated rule checking, clash resolution, and fabrication-oriented information exchange.

Author Contributions: Conceptualization, S.L. and Q.L.; methodology, Y.L., Q.L. and H.L.; software, Q.L.; validation, Q.L. and H.L.; formal analysis, Q.L.; investigation, Q.L.; resources, S.L. and Q.L.; data curation, Q.L. and H.L.; writing—original draft preparation, Y.L. and Q.L.; writing—review and editing, S.L. and Q.L.; visualization, Q.L.; supervision, S.L.; project administration, Q.L.; funding acquisition, S.L. All authors have read and agreed to the published version of the manuscript.

Funding: This research was funded by the National Natural Science Foundation of China (No. 52179133, No. U1404526).

Institutional Review Board Statement: Not applicable.

Informed Consent Statement: Not applicable.

Data Availability Statement: The data supporting the findings of this study are presented within the article. Relevant implementation details of the proposed workflow are also described in the article.

Conflicts of Interest: The authors declare no conflict of interest.

References

1. Faraji, A.; Homayoon Arya, S.; Ghasemi, E.; Soleimani, H.; Rahnamayiezekavat, P. A Constructability Assessment Model Based on BIM in Urban Renewal Projects in Limited Lands. *Buildings* **2023**, *13*, 2599. [CrossRef]
2. Belcher, E.J.; Abraham, Y.S. Lifecycle Applications of Building Information Modeling for Transportation Infrastructure Projects. *Buildings* **2023**, *13*, 2300. [CrossRef]
3. Khattra, S.K.; Rai, H.S.; Singh, J. Towards Automated Structural Stability Design of Buildings—A BIM-Based Solution. *Buildings* **2022**, *12*, 451. [CrossRef]
4. Zheng, C.; Yi, C.; Lu, M. Integrated optimization of rebar detailing design and installation planning for waste reduction and productivity improvement. *Autom. Constr.* **2019**, *101*, 32–47. [CrossRef]
5. Li, S.; Shi, Y.; Hu, J.; Li, S.; Li, H.; Chen, A.; Xie, W. Application of BIM to Rebar Modeling of a Variable Section Column. *Buildings* **2023**, *13*, 1234. [CrossRef]
6. Yang, L.; Gao, X.; Chen, S.; Li, Q.; Bai, S. A 3D Parameterized BIM-Modeling Method for Complex Engineering Structures in Building Construction Projects. *Buildings* **2024**, *14*, 1752. [CrossRef]
7. Zou, Y.; Hu, F.; Yang, H.; Cai, J.; Pan, H.; Zhang, Q. Detailed Design of Special-Shaped Steel Structures Based on DfMA: The BIM-FEM Model Conversion Method. *Buildings* **2024**, *14*, 1320. [CrossRef]
8. Madiniyeti, J.; Zhou, Q.; Qi, H.; Chao, Y.; Zhang, Y. Research on automated modeling technology of sluice gate project based on BIM technology. *Sensors* **2024**, *24*, 5114. [CrossRef] [PubMed]
9. Li, S.; Li, S.; Hu, J.; Shi, Y.; Li, H.; Chen, A.; Xie, W. Intelligent Modeling of Edge Components of Prefabricated Shear Wall Structures Based on BIM. *Buildings* **2023**, *13*, 1252. [CrossRef]
10. Zhang, F.; Shen, Y.; Tan, L.; Jin, R.; Han, Y. Research on Self-Adaptive Reinforcement Plug-in of Prefabricated Concrete Component Based on BIM. *KSCE J. Civ. Eng.* **2024**, *28*, 2588–2599. [CrossRef]
11. Collao, J.; Lozano-Galant, F.; Lozano-Galant, J.A.; Turmo, J. BIM Visual Programming Tools Applications in Infrastructure Projects: A State-of-the-Art Review. *Appl. Sci.* **2021**, *11*, 8343. [CrossRef]
12. Li, H.; Zhang, E.; Liu, Q.; Li, S. Parameterized Layout Method of Spiral Hoop Rebar in Bridge Pier Base on BIM. *Buildings* **2026**, *16*, 426. [CrossRef]
13. Mangal, M.; Cheng, J.C.P. Automated Optimization of Steel Reinforcement in RC Building Frames Using Building Information Modeling and Hybrid Genetic Algorithm. *Autom. Constr.* **2018**, *90*, 39–57. [CrossRef]
14. Eleftheriadis, S.; Duffour, P.; Stephenson, B.; Mumovic, D. Automated Specification of Steel Reinforcement to Support the Optimisation of RC Floors. *Autom. Constr.* **2018**, *96*, 366–377. [CrossRef]
15. Liu, J.; Xu, C.; Wu, Z.; Chen, Y.F. Intelligent Rebar Layout in RC Building Frames Using Artificial Potential Field. *Autom. Constr.* **2020**, *114*, 103172. [CrossRef]
16. Liu, J.; Liu, P.; Feng, L.; Wu, W.; Li, D.; Chen, Y.F. Automated Clash Resolution for Reinforcement Steel Design in Concrete Frames via Q-Learning and Building Information Modeling. *Autom. Constr.* **2020**, *112*, 103062. [CrossRef]
17. Liu, J.; Li, S.; Xu, C.; Wu, Z.; Ao, N.; Chen, Y.F. Automatic and Optimal Rebar Layout in Reinforced Concrete Structure by Decomposed Optimization Algorithms. *Autom. Constr.* **2021**, *126*, 103655. [CrossRef]
18. Xu, C.; Liu, J.; Wu, Z.; Chen, Y.F. Automated Steel Reinforcement Detailing in Reinforced Concrete Frames Using Evolutionary Optimization and Artificial Potential Field. *Autom. Constr.* **2022**, *138*, 104224. [CrossRef]
19. Li, M.; Liu, Y.; Wong, B.C.L.; Gan, V.J.L.; Cheng, J.C.P. Automated Structural Design Optimization of Steel Reinforcement Using Graph Neural Network and Exploratory Genetic Algorithms. *Autom. Constr.* **2023**, *146*, 104677. [CrossRef]
20. Mangal, M.; Li, M.; Gan, V.J.L.; Cheng, J.C.P. Automated Clash-Free Optimization of Steel Reinforcement in RC Frame Structures Using Building Information Modeling and Two-Stage Genetic Algorithm. *Autom. Constr.* **2021**, *126*, 103676. [CrossRef]
21. Liu, P.; Qi, H.; Liu, J.; Feng, L.; Li, D.; Guo, J. Automated Clash Resolution for Reinforcement Steel Design in Precast Concrete Wall Panels via Generative Adversarial Network and Reinforcement Learning. *Adv. Eng. Inform.* **2023**, *58*, 102131. [CrossRef]
22. Ren, K.; Jia, L.; Huang, J.; Wu, M. Research on cutting stock optimization of rebar engineering based on building information modeling and an improved particle swarm optimization algorithm. *Dev. Built Environ.* **2023**, *13*, 100121. [CrossRef]
23. Sampaio, A.Z.; Gomes, A.M. BIM Structural Project Applied in a Case Study: Interoperability Analyses, Reinforcement Detailing Drawings and Quantity Take-Off. *Open Constr. Build. Technol. J.* **2021**, *15*, 196–213. [CrossRef]
24. Gomes, A.M.; Azevedo, G.; Sampaio, A.Z.; Sánchez-Lite, A. BIM in Structural Project: Interoperability Analyses and Data Management. *Appl. Sci.* **2022**, *12*, 8814. [CrossRef]
25. Aram, S.; Eastman, C.; Sacks, R. Requirements for BIM Platforms in the Concrete Reinforcement Supply Chain. *Autom. Constr.* **2013**, *35*, 1–17. [CrossRef]
26. Maciel, A.R.; Corrêa, F.R. Interoperability with IFC in the Automated Rebar Fabrication. In *Proceedings of the 33rd International Symposium on Automation and Robotics in Construction, Auburn, AL, USA, 18–21 July 2016*; International Association for Automation and Robotics in Construction (IAARC): Auburn, AL, USA, 2016; pp. 872–880. [CrossRef] [PubMed]

27. Maciel, A.R.; Corrêa, F.R. IFC-Based Cut and Bent Rebar Supply Chain Integration. In *Proceedings of the 34th International Symposium on Automation and Robotics in Construction, Taipei, Taiwan, 28 June–1 July 2017*; International Association for Automation and Robotics in Construction (IAARC): Taipei, Taiwan, 2017; pp. 140–147. [CrossRef] [PubMed]
28. Du, S.; Teng, F.; Zhuang, Z.; Zhang, D.; Li, M.; Li, H.; Weng, Y. A BIM-Enabled Robot Control System for Automated Integration between Rebar Reinforcement and 3D Concrete Printing. *Virtual Phys. Prototyp.* **2024**, *19*, e2332423. [CrossRef]
29. Kossakowski, P.G. Visual Programming as Modern and Effective Structural Design Technology—Analysis of Opportunities, Challenges, and Future Developments Based on the Use of Dynamo. *Appl. Sci.* **2023**, *13*, 9298. [CrossRef]
30. Seghier, T.E.; Khosakitchalert, C.; Liu, Z.; Ohueri, C.C.; Lim, Y.-W.; Zainazlan, A.F.B. From BIM to Computational BIM: A Systematic Review of Visual Programming Application in Building Research. *Ain Shams Eng. J.* **2025**, *16*, 103173. [CrossRef]
31. Solihin, W.; Eastman, C. Classification of Rules for Automated BIM Rule Checking Development. *Autom. Constr.* **2015**, *53*, 69–82. [CrossRef]
32. Khant, L.P.; Widjaja, D.D.; Kim, D.; Rachmawati, T.S.N.; Kim, S. Optimizing Rebar Process and Supply Chain Management for Minimized Cutting Waste: A Building Information Modeling-Based Data-Driven Approach. *Buildings* **2025**, *15*, 844. [CrossRef]
33. Rahimi, Z.; Maghrebi, M. Minimizing Rebar Cost Using Design and Construction Integration. *Autom. Constr.* **2023**, *147*, 104701. [CrossRef]
34. Eastman, C.; Lee, J.M.; Jeong, Y.S.; Lee, J.K. Automatic Rule-Based Checking of Building Designs. *Autom. Constr.* **2009**, *18*, 1011–1033. [CrossRef]
35. Widjaja, D.D.; Rachmawati, T.S.N.; Kim, S. A BIM-Based Intelligent Approach to Rebar Layout Optimization for Reinforced Concrete Columns. *J. Build. Eng.* **2025**, *99*, 111604. [CrossRef]
36. Khant, L.P.; Widjaja, D.D.; Kwon, K.; Kim, S. A BIM-Based Bar Bending Schedule Generation Algorithm with Enhanced Accuracy. *Buildings* **2024**, *14*, 1207. [CrossRef]
37. Wang, D.; Hu, Y. Research on the Intelligent Construction of the Rebar Project Based on BIM. *Appl. Sci.* **2022**, *12*, 5596. [CrossRef]
38. Chen, B.; Jiang, S.; Qi, L.; Su, Y.; Mao, Y.; Wang, M.; Cha, H.S. Design and Implementation of Quantity Calculation Method Based on BIM Data. *Sustainability* **2022**, *14*, 7797. [CrossRef]
39. Liu, Y.; Li, M.; Wong, B.C.L.; Chan, C.M.; Cheng, J.C.P.; Gan, V.J.L. BIM-BVBS Integration with openBIM Standards for Automatic Prefabrication of Steel Reinforcement. *Autom. Constr.* **2021**, *125*, 103654. [CrossRef]
40. Porwal, A.; Hewage, K.N. Building Information Modeling-Based Analysis to Minimize Waste Rate of Structural Reinforcement. *J. Constr. Eng. Manag.* **2012**, *138*, 943–954. [CrossRef]
41. Khondoker, M.T.H. Automated Reinforcement Trim Waste Optimization in RC Frame Structures Using Building Information Modeling and Mixed-Integer Linear Programming. *Autom. Constr.* **2021**, *124*, 103599. [CrossRef]
42. Widjaja, D.D.; Kim, S. Reducing Rebar Cutting Waste and Rebar Usage of Beams: A Two-Stage Optimization Algorithm. *Buildings* **2023**, *13*, 2279. [CrossRef]
43. Widjaja, D.D.; Lim, J.; Kim, S. Integrating Digital Twin and BIM for Special-Length-Based Rebar Layout Optimization in Reinforced Concrete Construction. *Buildings* **2025**, *15*, 2617. [CrossRef]
44. *JGJ 149-2017*; Technical Specification for Concrete Structures with Specially Shaped Columns. China Architecture & Building Press: Beijing, China, 2017.
45. *20G331-1*; Structural Construction of Concrete Shaped Columns. China Planning Press: Beijing, China, 2020.

Disclaimer/Publisher's Note: The statements, opinions and data contained in all publications are solely those of the individual author(s) and contributor(s) and not of MDPI and/or the editor(s). MDPI and/or the editor(s) disclaim responsibility for any injury to people or property resulting from any ideas, methods, instructions or products referred to in the content.